Korean J. Chem. Eng., 33(3), 831-837 (2016)
DOI: 10.1007/s11814-015-0234-4

pISSN: 0256-1115
eISSN: 1975-7220

Conversion of methanol into light olefins over ZSM-11 catalyst in a circulating fluidized-bed unit

Xiaojing Meng*,†, Huiwen Huang*, Qiang Zhang*, Minxiu Zhang*, Chunyi Li*, and Qiukai Cui**

*State Key Laboratory of Heavy Oil Processing, China University of Petroleum (East China), Qingdao 266555, Shandong, China
**Dagang Petrochemical Company, PetroChina Corporation, Tianjin 300280, P. R. China
(*Received 12 August 2015 • accepted 6 November 2015*)

Abstract−Methanol conversion and the reaction pathway were investigated in a pilot-scale circulating fluidized-bed (CFB) unit over hierarchical ZSM-11 catalyst. Experimental results indicated that ZSM-11 catalyst was highly resistant to external coke due to the formation of mesopores. Elevated temperatures favored the production of propylene and butylene and decreased the yield of ethylene. Additionally, no direct relations were shown between the formation of ethylene and other products under different pressures, suggesting that ethylene was a primary product produced at the initial of the reaction. Methylation-cracking and oligomerization were verified as the main reaction pathway for the formation of C_3^+ alkenes., Methylation and oligomerization of olefins were dominated under high methanol partial pressure and consequently responsible for the production of higher olefins, while the b-scission of $C_7^=$ for propene and butylene, and $C_8^=$ for butylene were enhanced at low methanol partial pressure.

Keywords: ZSM-11 Catalyst, Methanol Conversion, Reaction Pathway, CFB Unit, Reaction Conditions

INTRODUCTION

Since the discovery of the methanol-to-gasoline reaction by Mobil Oil [1], the methanol-to-hydrocarbon (MTHC) technology, mainly the methanol-to-gasoline (MTG) and methanol-to-olefin (MTO) reactions, has been regarded as a competitive route to upgrade any gasifiable carbon-rich feedstock, such as natural gas, coal, and biomass into value added products [2]. This technology is versatile, depending on the catalyst and process conditions, and the product can be light alkenes or high-octane gasoline. ZSM-5 and SAPO-34 are two archetypical catalysts for this process and are regarded as the most effective catalysts [3-5].

Mechanistic investigations of methanol conversion have already been done widely. There have been at least 20 distinct mechanisms proposed for methanol catalysis [6]. Experimental [7,8] and theoretical [9-11] work have shown that direct methanol coupling does not occur because of the unstable intermediates and high activation energy barriers. Then olefin methylation and cracking route was proposed by Dessau [12]. In this route, olefins are consecutively methylated by methanol, leading to the formation of higher olefins, which can then be cracked into light olefins. Then, another indirect route, known as hydrocarbon pool mechanism, came to attract much more attention [13]. The fundamental feature of this mechanism is that the certain organic active centers, known as hydrocarbon pool species (methylbenzenes), serve as co-catalysts within the pore of zeolites, to which methanol is added and olefins are eliminated [14,15]. Recently, a dual-cycle concept was proposed by Bjørgen [16]. In this concept, ethylene is formed from the lower methylbenzenes followed by re-methylation, and a methylation/cracking cycle involving only the C_3^+ alkenes. Whereas, for a given catalyst topology or a given set of conditions, the contribution of each cycle can be altered, showing that the aromatic- and olefin-based cycles can be propagated to different extents depending on the reaction conditions and catalyst properties [17].

Recently, our research group synthesized a hierarchical ZSM-11 zeolite with intercrystalline mesoporous and rod-like crystals intergrowth morphology through a simple and low-cost method [18,19]. This material has been successfully applied for industrial development, and the derivatives display an excellent activity in numerous catalytic processes [20-24]. ZSM-11 has been well-acknowledged to possess a fairly bigger cavity volume and lower sinuosity than ZSM-5 [25]. As a consequence, ZSM-11 is more favorable than ZSM-5 for the generation and diffusion of big molecules. Mesopores and nano-rods in ZSM-11 are also likely to shorten the diffusion path. A unique product distribution of methanol conversion under different operation conditions and a proposed pathway for ethylene and propylene formation on this special structured material in a circulating fluidized-bed unit was provided.

MATERIAL AND METHODS

1. Catalyst Preparation

Hierarchical ZSM-11 zeolite was prepared basically according to the method described in the literature [18]. The molar composition of the hierarchical ZSM-11 zeolites mixture was 9.0 Na_2O: 1.0 Al_2O_3: 65 SiO_2: 0.53 $(TBA)_2O$: 1300 H_2O. The product was filtered, washed, and dried at 110 °C overnight. The parent zeolites were turned into the H-form by three consecutive ion exchanges in 1 M

†To whom correspondence should be addressed.
E-mail: mengxiaojing88@126.com

NH_4NO_3 solution with a solution/zeolite ratio of 10 mL/g at 80 °C for 2 h.

Catalysts were prepared with kaolin, zeolite and colloidal silica as a binder (40 wt% silica was obtained from Qingdao Haiyang Chemical Co. Ltd. China). Kaolin was provided by China Kaolin Clay Co. Ltd. The shaped catalyst was prepared by spray granulation. The composition of catalysts was 35 wt% H-zeolite, 5 wt% silica and 60 wt% kaolin clay.

2. Catalyst Characterization

Bulk crystalline phases of the catalysts were determined by X-ray diffraction (XRD) on Philips X'Pert PRO MPD diffractometer (PANalytical Company, Netherlands) using Cu Kα radiation (40 kV, 40 mA) in the range between 3° and 75° with a step of 0.02°. Morphology and structure of the solids were investigated with scanning electron microscope S-4800 (Hitachi Company, Japan) after being sonified in ethanol. Textural parameters of the samples were determined by nitrogen adsorption isotherms, which were recorded at −196 °C using Quantachrome Autosorb iQ apparatus. The amounts of external and internal coke within the catalyst were estimated by combining the information from TGA and gas adsorption measurements. TGA gave the total amount of coke (external+internal), and it is assumed that the reduction in micropore volume from the gas adsorption measurements relative to the fresh samples corresponds to the amount of internal coke by assuming a coke density of 1.22 g/cm^3 [26]. The remaining amount of coke (found by subtraction) was then assumed to be external.

3. Experimental Apparatus

A schematic of the pilot-scale CFB unit is presented in Fig. 1. The unit mainly consists of a reactor (with a length of 1 m and an inner diameter of 92 mm) coupled with a disengager, a regenerator, and a delivering riser, as well as product recovery systems. During the tests, methanol was introduced into the bottom of the reactor through a pump at a certain flow rate, flowing upward and contacting the catalysts (mean diameter of 75 μm) with carrying of nitrogen (320 L/h) under atmospheric pressure. After the reaction, the mixture of products and catalysts was separated in the disengager; where the gaseous products were collected. The spent catalysts were transferred into the regenerator through the delivering riser to burn off the coke in the air at 650 °C, and the flow rate of the main air was 550 L/h.

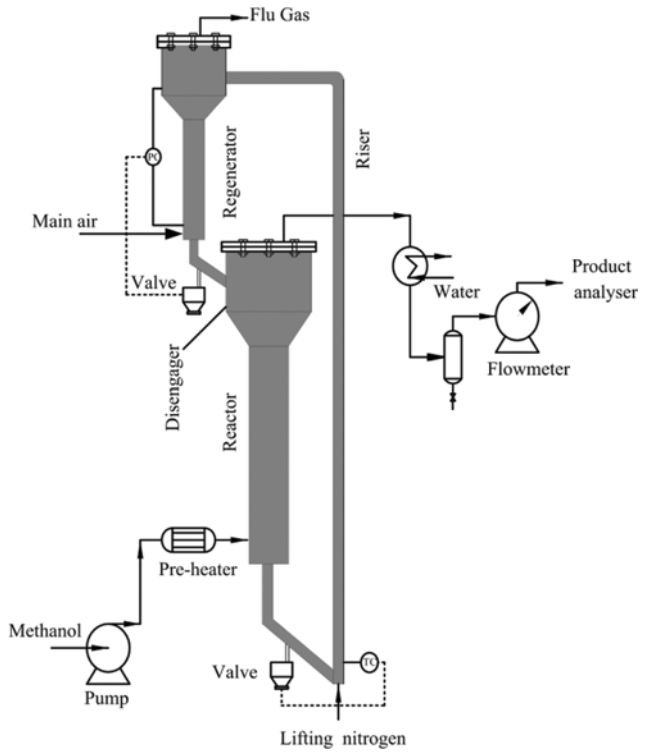

Fig. 1. Schematic diagram of the pilot-scale CFB unit.

4. Product Analysis

The composition of gaseous products was analyzed by using a Bruker 450-GC gas chromatograph (GC) with a TCD detector to analyze content of hydrogen, nitrogen and carbon oxide, and a FID detector column to determine the composition of hydrocarbons. The gasoline was analyzed on a Perkin Elmer Clarus 580 gas chromatograph (GC). Liquid products were analyzed on Agilent 6820 gas chromatograph (GC) equipped with HP-INNOWAX capillary column (30 m×0.32 mm×0.25 μm) and a flame ionization detector (FID) using ethanol as an internal standard.

The conversion of methanol and the product yield can be calculated by applying the mass balance between the inlet and outlet of the reactor as Eq. (1) and Eq. (2), respectively.

$$\text{Methanol Conversion} = \left(1 - \frac{m^o_{MEOH} + m^o_{DME}}{m^i_{MEOH}}\right) \times 100 \quad (1)$$

$$\text{Product Yield} = \left(1 - \frac{m^o_{CxHy}}{m^i_{MEOH}}\right) \times 100 \quad (2)$$

Superscript i refers to the components at the inlet of reactor, and superscript o refers to the components at the reactor outlet; subscript x refers to the number of carbon atoms.

RESULTS AND DISCUSSION

1. Catalyst Characterization

XRD was used to investigate the phase composition of samples.

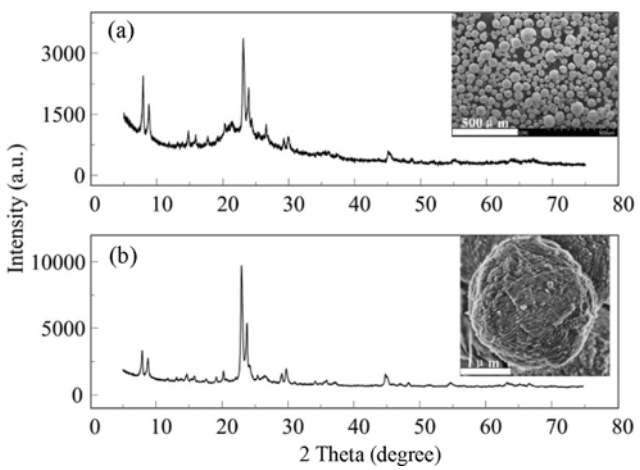

Fig. 2. XRD patterns and SEM images: (a) ZSM-11 catalyst; (b) ZSM-11 zeolite.

As shown in Fig. 2, ZSM-11 zeolite and catalyst both exhibited representative XRD patterns of a fully crystalline MEL structure, with two characteristic diffraction peaks indexed to the [501] and [303] crystal planes [27]. The morphology and mean size of the crystallites obtained by SEM were also presented in Fig. 2. The zeolite was composed of considerable nanorods which grafted and aggregated together to form spheroidal particles about 1.5-2 μm in diameter.

2. Reaction Performance over ZSM-11 Catalyst

The reaction performance and stability were evaluated under reaction conditions that reaction temperature was 500 °C with nitrogen as carrier gas (no catalyst regeneration), and residence time was 7.94 s.

The pilot-scale evaluation in this CFB unit lasted for 30 h, and the results are illustrated in Fig. 3. It was clear that the activity of ZSM-11 catalyst maintained a high level under present reaction conditions, confirming that with an appropriate contact time in continuous-flow condition, the high activity on ZSM-11 catalyst could be kept for a long time. Before 25 h on stream, propylene and butylene were the main products and their yield varied slightly from 14.0 wt% and 7.95 wt% to 17.06 wt% and 8.65 wt%, respectively. At the same time, the ethylene yield was in the range of 4.3-5.5 wt%. Note that the methanol conversion and yield of ethylene were not significantly changed with prolonging the reaction time before 30 h, while the yield of propylene and butylene decreased slightly after 25 h, implying that propylene and butylene were more sensitive to coke.

It is well established that mesoporous catalysts display improved lifetime or resistance toward deactivation in the MTH reaction. Thus, our initial hypothesis was that the ZSM-11 zeolite would be resistant toward deactivation due to a higher tolerance for external coke as a consequence of mesopore formation. This notion was examined further in Fig. 4, where the coke deposits were subdivided into internal and external coke, based on the thermo-gravimetric and gas adsorption measurements [26]. As seen, after 30 h, the catalyst accommodated a large amount of external coke. This indicated that external coke might play an essential role in the de-

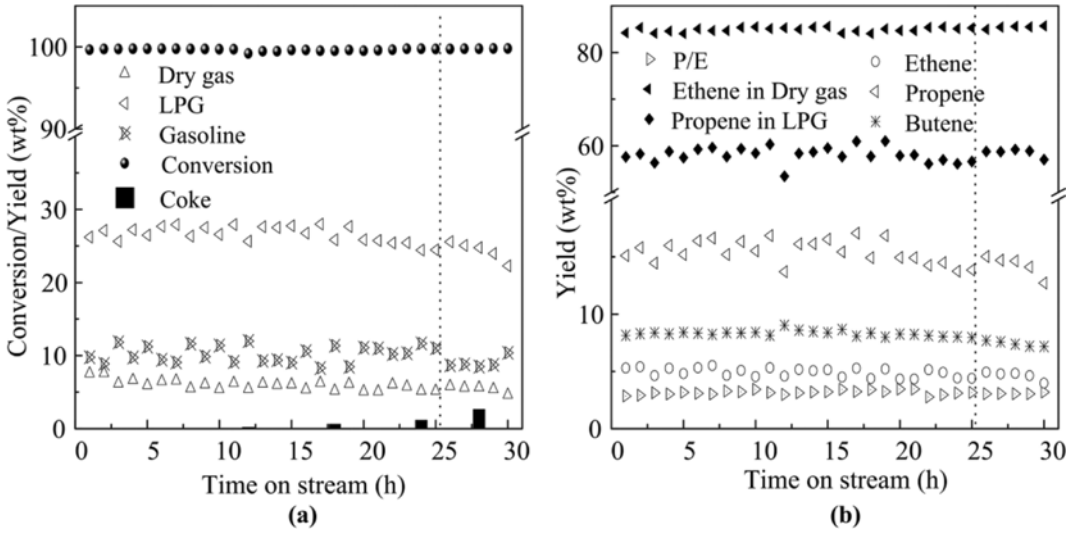

Fig. 3. Effect of coke content for methanol conversion, reaction temperature of 500 °C and residence time of 7.94 s: (a) Product distribution and conversion; (b) main products yield and P/E.

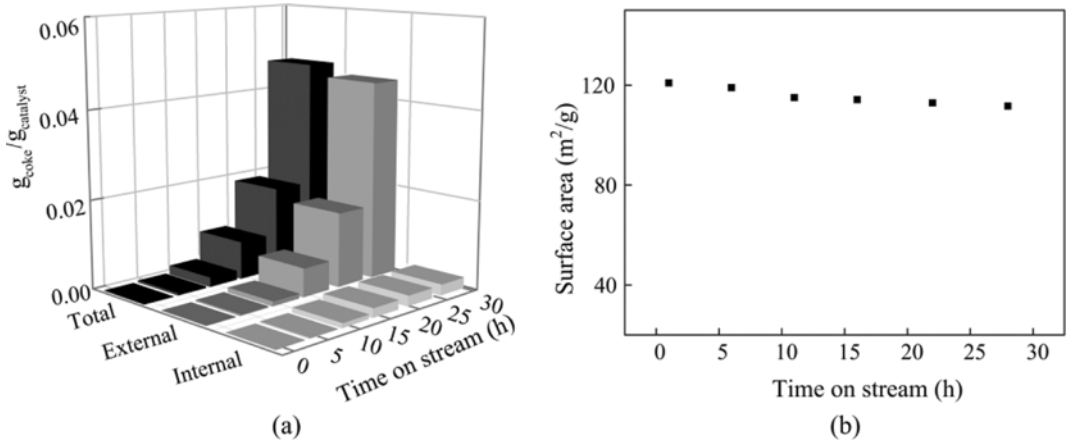

Fig. 4. The distribution of the total (black), internal (dark gray) and external (pale gray) amount of coke (a) and surface area (b) of ZSM-11 catalyst with time on stream.

Table 1. Catalytic performance of methanol on different catalysts

Catalysts	ZSM-5	ZSM-11
Conversion (wt%)	99.98	93.09
	Yield (wt%)	
C_2H_4	2.25	5.96
C_3H_6	2.55	7.47
C_4HTI	0.78	0.46
Dry gas	2.94	6.26
LPG	18.68	17.01
Gasoline	20.91	18.33
Coke	0.46	0.20
Ethylene in dry gas	76.56	95.24
Propylene in LPG	13.65	43.91
P/E	1.13	1.25

activation of the catalyst, and the formation of mesopores might affect the distribution of coke deposits (external versus internal). It was tempting to link the coke among the ZSM-11 catalyst to an increased mobility of coke and coke precursors, suggesting that porosity played an important role for the improved deactivation behavior of ZSM-11 catalyst, as also suggested previously [28].

The MTO reactions on conventional ZSM-5 and ZSM-11 catalysts with the same Si/Al ratio were carried out at 673 K (Table 1). The results showed that under this condition, the converting ability of ZSM-11 catalyst was lower than that of ZSM-5 catalyst, which may be due to its weaker acidity (0.325 and 0.229 mmol/g for ZSM-11 and ZSM-5 catalyst, respectively). However, the yield of ethylene and propylene was significantly higher for ZSM-11 catalyst. For the conventional ZSM-5 catalyst, the larger amount of acid sites led to higher hydrogen-transfer ability, and thus the selectivity of light olefins was lower.

3. Effect of Temperature

The effect of temperature on methanol conversion has been studied widely [6,29]. Wu found that product distribution was remarkably affected by operation conditions only at low methanol conversions (<80%). When methanol conversion approaches 100%, product distribution is hardly affected by operation conditions [30]. Whereas, Chang monitored that at higher temperatures, the olefin formation was favored with respect to the formation of aromatics [31].

To simulate the operation of a commercial MTO unit, experiments were carried out under a fixed regenerated catalyst temperature of 650 °C, while the reaction temperature was elevated from 350 °C to 550 °C. The results are displayed in Fig. 5.

In this study, the conversion at different temperatures was constantly higher than 90 wt%, showing that ZSM-11 catalysts processed an excellent methanol converting ability. When the temperature increased from 350 °C to 450 °C, the yield of propylene, butylene, and gasoline increased from 7.06 wt%, 3.63 wt%, and 17.53 wt% to 9.23 wt%, 5.87 wt%, and 18.23 wt%, as shown in Fig. 5, respectively, while ethylene yield declined abruptly from 8.87 wt% to about 4.6 wt%. With the temperature increasing on (>450 °C), the yield for propylene, butylene and ethylene displayed similar behavior as at low temperatures. A maximum yield to gasoline was achieved at about 450 °C.

It is generally acknowledged that yield of propylene is enhanced at higher temperature (450-500 °C). In this study, this viewpoint was valid at any methanol conversion, and the increase of propylene and butylene yield might be due to cracking of higher olefins. Notably, the yield of ethylene decreased with increasing temperature. Van Rensburg et al. [32] concluded that at low conversion and/or low temperature, ethylene was mainly a residual primary reaction product. At higher temperatures (>400 °C), however, ethylene was a product resulting from secondary cracking [28]. As displayed in Fig. 5, ethylene was abundant at low temperature (350 °C). As the temperature increased (<500 °C), ethylene became of minor importance and butylene and especially propylene became more dominated, therefore leading to a substantial increase of propylene to ethylene (P/E) ratio. In addition, thermal cracking occupied a higher fraction at much higher reaction temperatures (>500 °C), consequently producing more by-products. Meanwhile, the hydrogen transfer and cyclization reaction were inhibited and aromatization was promoted, as reflected by an increase of aromatics and the decline of paraffins and naphthenes in gasoline (Fig. 5(b)). Note that the change of components' content in gasoline in this paper was the same as the yield in the product, which was not listed here.

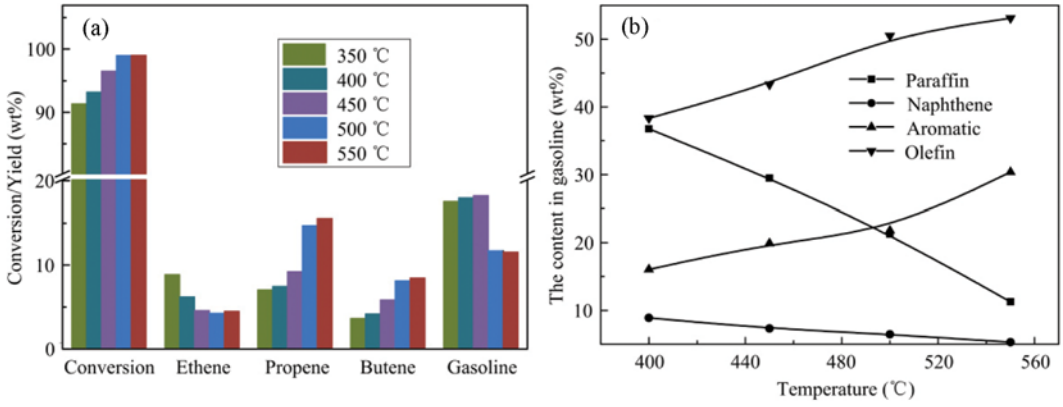

Fig. 5. Effect of reaction temperature in methanol conversion over ZSM-11 catalyst: (a) Conversion and main products; (b) the composition of gasoline.

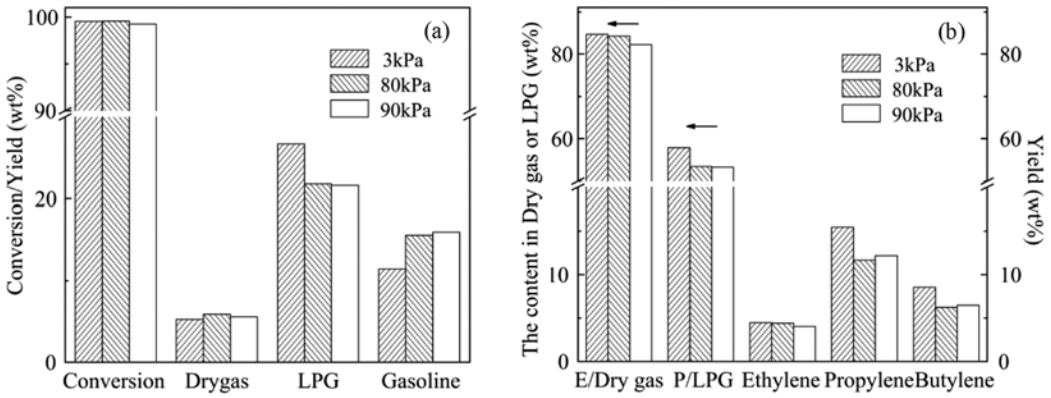

Fig. 6. Effect of pressure on methanol conversion over ZSM-11 catalyst, reaction temperature of 500 °C: (a) Product distribution and conversion; (b) main products yields.

4. Effect of Pressure

In the conversion of methanol, the product distribution can be markedly influenced by the reactant partial pressure. In the methanol to gasoline process, Chang et al. found that elevated pressures tended to enhance secondary alkylation reactions that resulted in the increase in the aromatic chain-to-ring ratio [33]. An eight-fold increase in selectivity towards light olefins occurred when the partial pressure of methanol was changed from 1 to 0.07 bar under the same residence time. In the present study, product distribution in methanol conversion were investigated at methanol partial pressure of 3, 80 and 90 kPa at 500 °C while keeping the residence time constant.

As seen in Fig. 6, methanol conversion was not notably changed with varying methanol partial pressures. When the partial pressure of methanol increased from 3 kPa to 80 kPa at complete methanol conversion, the yield of LPG decreased sharply from 26.7 wt% to 21.8 wt%, while that of gasoline was increased; only dry gas almost remained unchanged. Meanwhile, the yield of propylene and butylene displayed a significant decrease as LPG, which was inconsistent with Wu [30], who found that $C_4^=$ and $C_5^=$ selectivity were not affected by methanol partial pressure but methanol conversion and only propylene selectivity were inhibited with increasing methanol partial pressure. The results here might indicate the different reaction pathways over ZSM-11 catalyst. With an increase in methanol

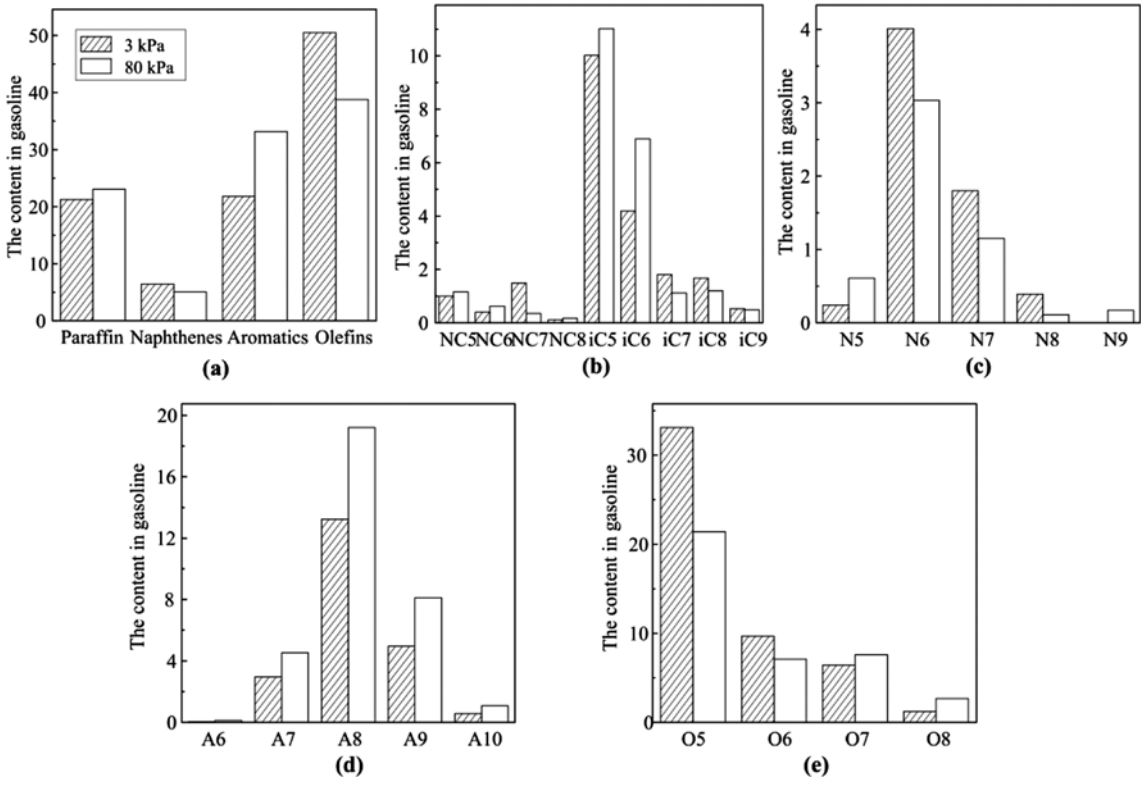

Fig. 7. Effect of pressure on the composition of gasoline over ZSM-11 catalyst, reaction temperature 500 °C: (a) Gasoline; (b) paraffins; (c) naphthenes; (d) aromatics; (e) olefins.

partial pressure, the yield of ethylene decreased slightly, confirming the limited interactions between ethylene with other light olefins. Moreover, the content of ethylene and propylene in dry gas and LPG showed a moderate decrease, duo to an increasing hydrogen transfer reaction with the increase of methanol partial pressure.

To find the formation paths of light olefins clearly here, we analyzed the change of gasoline composition. As shown in Fig. 7, a remarkable change was observed from the composition of gasoline at methanol partial pressure of 3 kPa and 80 kPa. With an increase of methanol partial pressure, the olefin content dropped sharply from 50 wt% to 38 wt%, while that of aromatics increased observably from 22 wt% to 33 wt%. Meanwhile, high methanol partial pressure tended to promote the formation of paraffins slightly, as well as alkanes in LPG, and the content of naphthenes decreased mildly.

For aromatics, C_8 aromatics were dominant, in which three xylenes were most abundant (o-xylene : m-xylene : p-xylene=17 : 50 : 33). Besides C_8 aromatics, C_9 and C_7 aromatics occupied a relatively smaller proportion, of which 1, 2, 4-trimethylbenzene and 1-methyl-3-ethylbenzene and toluene were the main components, respectively. The decrease of partial pressure of methanol tended to enhance the olefin formation and suppressed the aromatization [33]. On account of that, all the aromatics exhibited a significant increase at different levels at high methanol partial pressure, which was mainly due to the aromatization of olefins.

With regard to olefins, however, $C_5^=$ was dominant. $C_5^=$ and $C_6^=$ decreased acutely especially $C_5^=$ with the increase of methanol partial pressure, while both $C_7^=$ and $C_8^=$ yield was enhanced, which revealed that the change of propylene and butylene seemed to be opposed to that of $C_7^=$ and $C_8^=$. At lower pressures, oligomerization and cracking reaction became dominant, leading to the cracking of $C_7^=$ and $C_8^=$ to $C_3^=$ and $C_4^=$ [13,34]. Cracking of $C_6^=$ and $C_5^=$ at low pressure was not distinct, due to the extremely high methylation activity of $C_4^=$ and $C_5^=$. From the results at different pressures, we could figure out that $C_6^=$ and $C_5^=$ were mainly formed from the methylation reactions, while $C_8^=$ was mainly formed from the olefin oligomerization reaction and the two kinds of reactions both contributed to the formation of $C_7^=$.

5. Possible Reaction Routes

In the hydrocarbon pool mechanism, ethylene was considered to be formed from the elimination of poly-methylated benzenes, which should be promoted at higher temperatures. Meanwhile, if the ethylene was the product of secondary reaction and produced from the cracking of higher alkenes, the yield of ethylene should also be enhanced when the temperature is increased. The two mechanisms both seemed to conflict with our result that the yield of ethylene dropped evidently with increased temperature. According to the thermodynamic analysis [30], the equilibrium composition of ethylene increased with a rise of temperature under a certain pressure. Hence, the effect of olefin oligomerization and cracking reaction on ethylene became more apparent only when the temperature was higher than 500 °C. Moreover, the yield of ethylene was almost not affected at different methanol partial pressures at 500 °C, when olefin oligomerization and cracking reactions were minor. That is, the production of ethylene almost had no direct and strong relations with other products and was only influenced greatly by temperature.

Therefore, we could reach the conclusion that ethylene was not formed from the secondary reactions and might be the primary product produced at the initial induction period, and the content of ethylene was determined by the temperature and was hardly affected by the pressure.

Moreover, it was notable that propene and butylene kept the same variation trend under different temperatures and pressures, making it rational that the formation of these two olefins might abide by the same reaction route. With the reaction temperature increasing, the cracking of gasoline was accelerated and favored the formation of light olefins. The activity of butylene methylation was higher than that of propylene, resulting in a slower increasing rate than propylene. Ethylene, propylene and butylene might be the primary products produced in the induction period, but the content and distribution of these olefins were not quite clear. Meanwhile, ethylene was not so activated with methanol as other olefins like propylene and butylene. Therefore, propylene and butylene were dominated with temperature increasing. Though the yield of gasoline decreased, the content of olefins and aromatics in gasoline still kept increasing for the enhanced aromatization and existence of methylation and cracking reactions between olefins (except ethylene).

It was found that the most abundant component in gasoline was $C_5^=$ at reaction temperature of 500 °C and methanol partial pressure of 3 kPa, implying a high methylation/cracking activity for butylene and relative low of $C_5^=$. Moreover, unlike the change of $C_5^=$ and $C_6^=$, $C_7^=$ and $C_8^=$ increased at methanol partial pressure of 80 kPa, which was reversed to the trend of propylene and butylene, showing that oligomerization of $C_3^=$ and $C_4^=$ to form $C_7^=$ and $C_8^=$ occurred at high pressure (80 kPa). As a result, we concluded that $C_6^=$ and $C_5^=$ were mainly formed through the methylation reaction, while the amount of $C_8^=$ was determined by the olefin oligomerization reaction, and the above two reactions both contributed to the formation of $C_7^=$ as discussed above. The oversimplified form of propylene production over ZSM-11 catalyst was represented by Scheme 1.

Nevertheless, though the proposed dominant pathways for propene could be used to model reactions over ZSM-11 catalyst, at longer residence time when methanol conversion approaches completion, the alkene inter-conversion reactions on the basis of oligomerization and cracking will become evident, and thus make the final alkene product mixture approach the chemical equilibrium composition. Furthermore, the side reactions of the alkenes to form paraffins and aromatics constituting the gasoline and LPG fractions will also take place to a modest extent. Exploring the exact

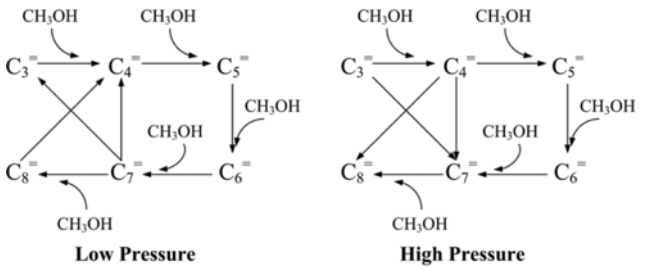

Scheme 1. Dominant reaction pathway for propene formation over ZSM-11 catalyst.

extent and the related reaction pathways of the side reactions were the aims of further studies which are already in progress.

CONCLUSIONS

Methanol conversion over a novel ZSM-11 catalyst in a pilot-scale CFB unit was investigated. The results demonstrated that product distribution and methanol conversion were affected slightly after 30 h on stream, and external coke was dominated for the decrease of hydrocarbons, whereas, the methanol partial pressure and the temperature generated significant influence on reaction performance.

As for ethylene, its yield dropped sharply when increasing temperature and was almost hardly influenced by methanol partial pressure, which revealed that ethylene was a primary product produced at the initial stage. Furthermore, it was notable that the change of propene and butylene kept resembled under different conditions. Higher reaction temperature favored the cracking of gasoline, and therefore enhanced the production of light olefins. At low pressures, oligomerization and cracking reaction became dominant, leading to cracking of $C_7^=$ and $C_8^=$ to form $C_3^=$ and $C_4^=$. It was proposed that $C_6^=$ and $C_5^=$ were mainly formed through the methylation reaction, and $C_8^=$ was mainly from the olefin oligomerization reaction, whereas the formation of $C_7^=$ was attributed to both two reactions above.

ACKNOWLEDGEMENT

The authors acknowledge financial support provided by the National 973 Program of China (No. 2012CB215006).

REFERENCES

1. C. D. Chang and A. J. Silvestri, *J. Catal.*, **47**, 249 (1977).
2. F. J. Keil, *Micropor. Mesopor. Mater.*, **29**, 49 (1999).
3. B. P. C. Hereijgers, F. Bleken, M. H. Nilsen, S. Svelle, K. P. Lillerud, M. Bjørgen, B. M. Weckhuysen and U. Olsbye, *J. Catal.*, **264**, 77 (2009).
4. H. A. Zaidi, and K. K. Pant, *Korean J. Chem. Eng.*, **27**, 1404 (2010).
5. H. G. Kim, K. Y. Lee, H. G. Jang, Y. S. Song and G. Seo, *Korean J. Chem. Eng.*, **27**, 1773 (2010).
6. M. StÖcker, *Micropor. Mesopor. Mater.*, **29**, 3 (1999).
7. W. Song, D. M. Marcus, H. Fu, J. O. Ehresmann and J. F. Haw, *J. Am. Chem. Soc.*, **124**, 3844 (2002).
8. D. M. Marcus, K. A. McLachlan, M. A. Wildman, J. O. Ehresmann, P. W. Kletnieks and J. F. Haw, *Angew. Chem. Int. Ed.*, **45**, 3133 (2006).
9. D. Lesthaeghe, V. V. Speybroeck, G. B. Marin and M. Waroquier, *Angew. Chem. Int. Ed.*, **45**, 1714 (2006).
10. S. R. Blaszkowski and R. A. van Santen, *J. Am. Chem. Soc.*, **119**, 5020 (1997).
11. D. Lesthaeghe, V. Van Speybroeck, G. B. Marin and M. Waroquier, *Ind. Eng. Chem. Res.*, **46**, 8832 (2007).
12. R. M. Dessau, *J. Catal.*, **99**, 111 (1986).
13. I. M. Dahl and S. Kolboe, *Catal. Lett.*, **20**, 329 (1993).
14. W. Song, J. F. Haw, J. B. Nicholas and C. S. Heneghan, *J. Am. Chem. Soc.*, **122**, 10726 (2000).
15. S. Ilias and A. Bhan, *J. Catal.*, **311**, 6 (2014).
16. M. Bjørgen, S. Svelle, F. Joensen, J. Nerlov, S. Kolboe, F. Bonino, L. Palumbo, S. Bordiga and U. Olsbye, *J. Catal.*, **249**, 195 (2007).
17. S. Ilias and A. Bhan, *J. Catal.*, **290**, 186 (2012).
18. Q. Yu, C. Cui, Q. Zhang, J. Chen, Y. Li, J. Sun, C. Li, Q. Cui, C. Yang and H. Shan, *J. Energy Chem.*, **22**, 761 (2013).
19. C. Li, Q. Yu and J. Chen, CN Patent, ZL 201210003750.5 (2012).
20. Y. Gu, N. Cui, Q. Yu, C. Li and Q. Cui, *Appl. Catal. A*, **429-430**, 9 (2012).
21. Q. Yu, X. Meng, J. Liu, C. Li and Q. Cui, *Micropor. Mesopor. Mater.*, **181**, 192 (2013).
22. Q. Yu, Q. Zhang, J. Liu, C. Li and Q. Cui, *CrystEngComm*, **15**, 7680 (2013).
23. Q. Yu, Y. Li, X. Meng, Q. Cui and C. Li, *Mater. Lett.*, **124**, 204 (2014).
24. Q. Yu, J. Chen, Q. Zhang, C. Li and Q. Cui, *Mater. Lett.*, **120**, 97 (2014).
25. L. Zhang, H. Liu, X. Li, S. Xie, Y. Wang, W. Xin, S. Liu and L. Xu, *Fuel Process. Technol.*, **91**, 449 (2010).
26. F. L. Bleken, K. Barbera, F. Bonino, U. Olsbye, K. P. Lillerud, S. Bordiga, P. Beato, T. V. W. Janssens and S. Svelle, *J. Catal.*, **307**, 62 (2013).
27. G. T. Kokotailo, P. Chu, S. L. Lawton and W. M. Meier, *Nature*, **275**, 119 (1978).
28. T. V. W. Janssens, *J. Catal.*, **264**, 130 (2009).
29. W. J. H. Dehertog and G. F. Froment, *Appl. Catal.*, **71**, 153 (1991).
30. W. Wu, W. Guo, W. Xiao and M. Luo, *Fuel Process. Technol.*, **108**, 19 (2013).
31. C. D. Chang, C. T. W. Chu and R. F. Socha, *J. Catal.*, **86**, 289 (1984).
32. L. J. Van Rensburg, R. Hunter and G. J. Hutchings, *Appl. Catal.*, **42**, 29 (1988).
33. C. D. Chang, W. H. Lang and R. L. Smith, *J. Catal.*, **56**, 169 (1979).
34. S. Teketel, U. Olsbye, K. P. Lillerud, P. Beato and S. Svelle, *Micropor. Mesopor. Mater.*, **136**, 33 (2010).